Geophys. J. R. astr. Soc. (1966) **12**, 33–54.

Measurements of the Orbital Velocities of Sea Waves and their Use in Determining the Directional Spectrum

K. F. Bowden and R. A. White

(Received 1966 March 28)

Summary

The three components of orbital velocity in sea waves approaching a shore have been measured using an electromagnetic flowmeter. The spectra of these components have been compared with the spectrum of the pressure oscillations recorded at the same time. From these data, the relations between the pressure and velocity components at various heights above the bottom have been investigated and have been compared with those given by first order potential wave theory. The spectra of the wave pressure and two horizontal velocity components have then been combined so as to yield an estimate of the directional spectrum of the waves. The method was found to work satisfactorily but, because of the complicated bottom topography near the site of these experiments (off the Gladstone Dock, Liverpool), the results obtained cannot be related to the properties of the waves in deeper water.

1. Introduction

The aim of the work described here was, firstly, to investigate the use of an electromagnetic flowmeter for measuring the three components of orbital velocity in sea waves and, secondly, to use simultaneous measurements of the two horizontal components, u and v, and the pressure p as a means of determining the directional spectrum. As a pre-requisite to the second objective, a study was made of the relations between the pressure and the velocity components and their dependence on depth.

Although a number of measurements have been made of the orbital velocities in waves generated in laboratory experiments, there have been comparatively few observations in natural waves. Among these, Inman & Nasu (1956) used the bending of a cylindrical rod, as measured by strain gauges, to determine orbital velocities near the sea bed. Lukasik & Grosch (1963) used a bead thermistor, operating on the principle of a hot-wire anemometer, to measure the velocity near the sea bed in ocean swell. Nagata (1961, 1964b, c) has used an electromagnetic current meter, in which the water flowed through a tube in a streamlined body, to study the orbital velocities below waves in shallow water and relate them to sediment transport. Nagata was also able (1964a, d) to estimate the direction of approach of the waves, under certain conditions, from the two horizontal components of orbital velocity, by identifying individual wave crests. In an alternative method, he used the spectra of the two components. Miller & Zeigler (1964) have measured the internal velocity field in breaking waves using an acoustic flowmeter and also a magnetic flowmeter, in which the water flowed through a straight tube passing through a fibreglass sphere.

Several methods have been described for determining the directional spectrum of waves in the open sea or approaching a coast. One of these makes use of stereophotographs of the sea surface, taken from the air, as in the Stereo Wave Observation Project (SWOP), described by Cote *et al.* (1960). In a second type of method, an array of detectors is used and the directional properties are inferred from the phase relations between the signals. The theoretical background has been reviewed by Barber (1963), and Munk *et al.* (1963) have used the method for the directional recording of swell arriving at a coast from distant storms. The third method involves measuring some property of the waves, such as the surface slope or the orbital velocity, which itself depends on the direction of propagation. Longuet-Higgins, Cartwright & Smith (1963) used a floating buoy to measure the elevation ζ and the two components of slope, $\partial\zeta/\partial x$ and $\partial\zeta/\partial y$, and hence derived the directional spectrum (see also Longuet-Higgins 1962). In a development of this technique, a higher resolution has been obtained by using a clover-leaf pattern of three buoys, which enabled the components of wave curvature $\partial^2\zeta/\partial x^2$ and $\partial^2\zeta/\partial y^2$, to be measured as well (Cartwright & Smith 1964). It was pointed out by Cartwright (1962) that the directional spectrum could be obtained in essentially the same way by measuring the pressure and two components of orbital velocity instead of the elevation and surface slopes. The use of this method was proposed by Nagata (1964a), who developed the theory in detail.

The instruments used in the present investigation were an electromagnetic flowmeter and a pressure gauge. These two instruments enabled measurements of the three components of orbital velocity and the pressure below the waves to be obtained. The records, which were in analogue form, were converted into digital time series and analysed by correlation and power spectra techniques. The observed relations between the components were compared with those derived from a simple theoretical model, representing a wave motion of small amplitude and employing a first order potential. This model was found to be a sufficiently good approximation and on this basis the data from the components on each record were combined to give a smoothed estimate of the directional spectrum.

2. Instrumental scheme (see Fig. 1)

The instruments used during the experiments are described briefly below.

(a) *Electromagnetic flowmeter.* This instrument is used to measure the components of water velocity by means of electromagnetic induction. Earlier descriptions of the instrument have been given by Bowden & Fairbairn (1956) and Howe (1960). A full account of the physical principles on which it is based was given by Longuet-Higgins & Barber (1946).

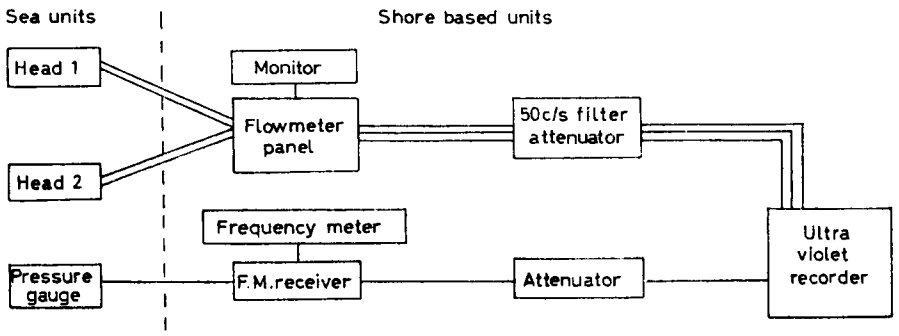

FIG. 1. The instrumental scheme.

The sea unit (see Fig. 2) consists of an oblate tufnol spheroid of 10 cm diameter containing a circular coil. When the unit is placed in moving water and alternating current is passed through the coil, electromotive forces are generated in the water. These are detected with electrodes suitably placed on the circumference of the spheroid. Voltage fluctuations arising from changes in the water veloicty past the measuring head can be isolated from spurious signals in the measuring head circuit and after suitable amplification can be fed into a recorder. Two sea units may be used to yield three components of water velocity fluctuations. The instrument was calibrated, in a water channel in the Fluid Mechanics Laboratory at Liverpool University, for water speeds from 0 to 60 cm/s.

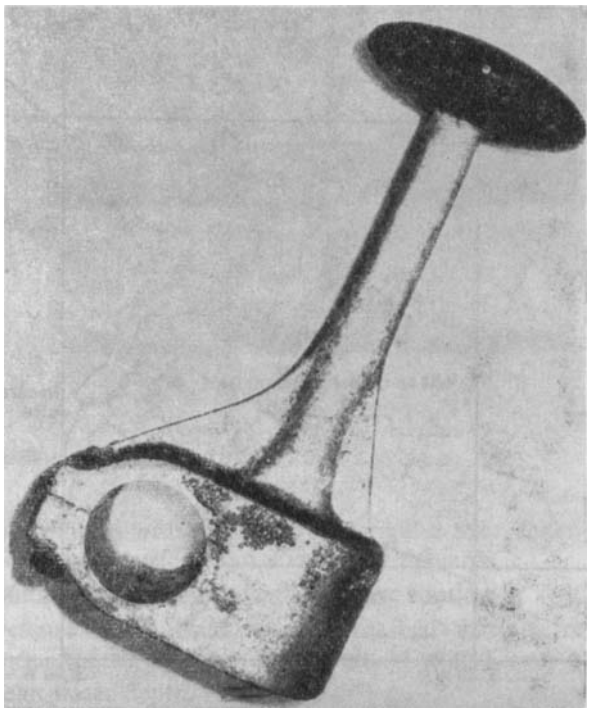

FIG. 2. Flowmeter sea-unit.

(b) *The frequency-modulated pressure gauge* was designed and constructed at the British National Institute of Oceanography. A complete account of this instrument is given by Harris & Tucker (1963). The sea-unit generates a signal whose frequency is dependent on the water pressure acting on it. This signal is passed to a frequency modulated receiver which gives an output proportional to the frequency and hence the pressure. The frequency from the sea unit may also be monitored directly to provide an estimate of the mean depth of the instrument below the water surface. The instrument was calibrated for depths of water between 0 and 9 m (30 ft) and the response was found to be nearly linear over this range.

(c) *The recorder.* The outputs from the electromagnetic flowmeters and the pressure gauge were recorded by galvanometers in a six-channel ultraviolet recorder, using photo-sensitive paper.

3. Experimental site and instrumental set-up

The site chosen for the experiment was just outside the Gladstone Dock situated at the mouth of the River Mersey (see Fig. 3). A gently sloping beach commences at the base of the Dock Wall and runs out to sea where the sand changes to mud and rocks in the Mersey Channel. The sand is exposed at low tide for distances of 50–100 m seaward of the wall.

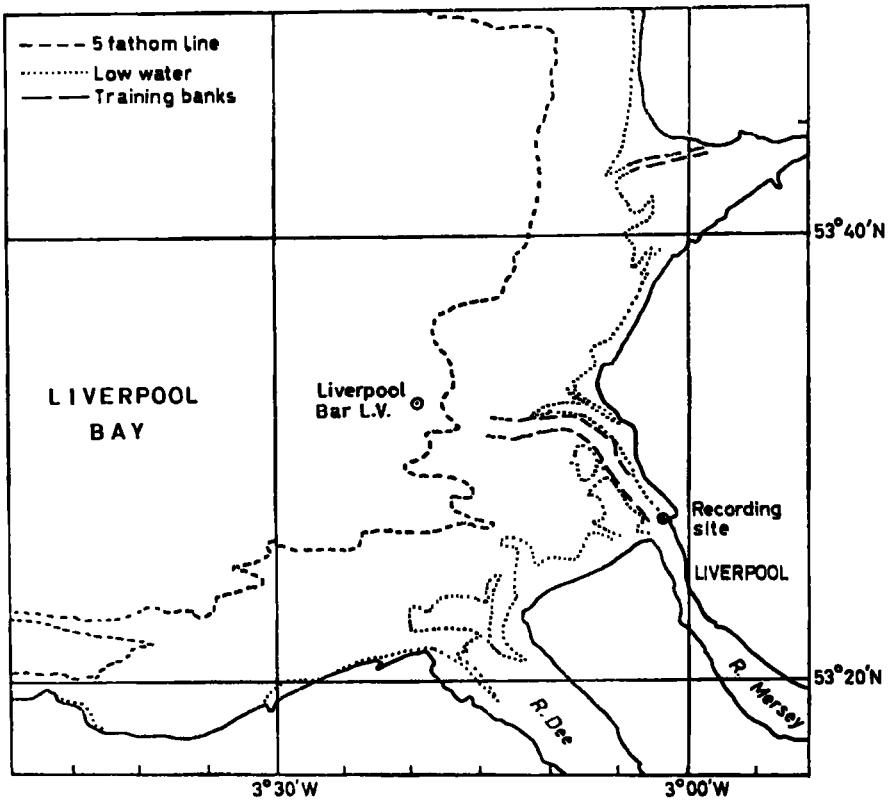

FIG. 3. Liverpool Bay, showing recording site.

The sea-units of the instruments were positioned on a 6 m (20 ft) scaffolding pole about 50 m from the Dock Wall (see Fig. 4). Cables were run up the shore to the electronic equipment which was housed in the Port Radar Station. The instrumental arrangement enabled simultaneous recordings of orbital velocity and sea-bed pressure to be obtained.

This site, although easily accessible, had the following inherent disadvantages:

(i) Wave recording was limited to days when the wind direction lay between west and north and when the tidal range was large.

(ii) A possibility existed of interference between the incoming waves and reflections off the sea wall.

(iii) General distortion of the incoming waves could be caused by the very uneven bottom topography of Liverpool Bay and interference from the tidal currents at the mouth of the Mersey.

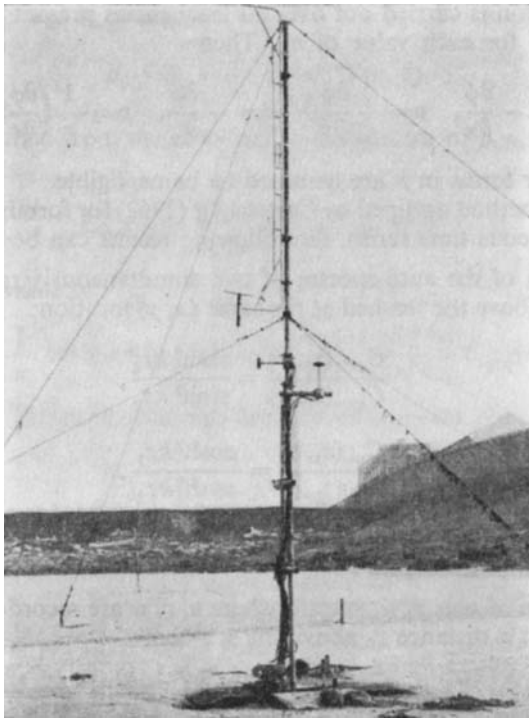

FIG. 4. Instrumental set-up at the site.

4. Theory applicable to the experiment

Notation

x, y, z	co-ordinates with respect to rectangular axes, taken with origin in the mean water surface and z vertically upwards.
u, v, w	orbital velocity components of wave motion in x, y, z directions.
p	pressure fluctuations on the sea-bed arising from surface waves (measured as an equivalent height of water).
d	mean water depth.
z_0, z_1, z_2	distances of instruments from the sea-bed.
C_{11}	auto-spectrum of series 1.
C_{12}	co-spectrum of series 1 and 2.
Q_{12}	quadrature-spectrum of series 1 and 2.
k	wave number ($= 2\pi$/wavelength).
σ	angular frequency ($= 2\pi$/period).
g	acceleration due to gravity.
ψ	$= kx\cos\theta + ky\sin\theta - \sigma t + \epsilon$.
θ	direction of propagation, measured from positive x direction.
ϵ	arbitrary phase angle.

If it is assumed that the wave motion in water of finite depth d may be represented by a first order velocity potential $\phi\ (x, y, z, t)$, then

$$\phi(x, y, z, t) = \sum_n \frac{g}{\sigma_n} A_n \frac{\cosh k_n(z+d)}{\cosh k_n d} \cos\psi_n,$$

where the summation is carried out over all frequencies present in the spectrum and $\sigma_n^2 = gk_n \tanh k_n d$ for each value of n. Then

$$u = -\frac{\partial \phi}{\partial x}, \quad v = -\frac{\partial \phi}{\partial y}, \quad w = -\frac{\partial \phi}{\partial z}, \quad p = \frac{1}{g}\left(\frac{\partial \phi}{\partial t}\right)_{z=-d},$$

where higher order terms in p are assumed to be negligible.

Following the method outlined by Cartwright (1962) for forming spectral quantities from two simultaneous time series, the following results can be derived.

(i) Comparison of the auto-spectra of two simultaneously recorded components at distances z_1, z_2 above the sea-bed at the same (x, y) location:

$$\frac{C_{ww}(z_1, \sigma)}{C_{ww}(z_2, \sigma)} = \frac{\sinh^2 kz_1}{\sinh^2 kz_2}, \tag{1}$$

$$\frac{C_{uu}(z_1, \sigma)}{C_{uu}(z_2, \sigma)} = \frac{\cosh^2 kz_1}{\cosh^2 kz_2}. \tag{2}$$

The above equations can be used in a comparison with the observed attenuation of u and w components with depth.

(ii) Comparison of p, u, v, w, spectra where u, v, w are recorded at the same (x, y) location as p but at a distance z_0 above the sea-bed:

$$\frac{C_{pp}(\sigma)}{C_{uu}(z_0, \sigma) + C_{vv}(z_0, \sigma)} = \left(\frac{\sigma}{gk}\frac{1}{\cosh kz_0}\right)^2, \tag{3}$$

$$\frac{C_{pp}(\sigma)}{C_{ww}(z_0, \sigma)} = \left(\frac{\sigma}{gk}\frac{1}{\sinh kz_0}\right)^2. \tag{4}$$

(iii) The coherency between two related series A and B, recorded simultaneously, may be defined by

$$\gamma^2(\sigma) = \frac{C_{AB}^2 + Q_{AB}^2}{C_{AA} C_{BB}}. \tag{5}$$

If the coherency is comparatively high (greater than 0·8, say), the transfer function $\mu(\sigma)$ between the two series is given approximately by

$$\mu^2(\sigma) \approx \frac{C_{AA}}{C_{BB}} \tag{6}$$

as in Cartwright, Tucker & Catton (1962). The phase shift ϕ is given by

$$\tan \phi(\sigma) = \frac{Q_{AB}}{C_{AB}}. \tag{7}$$

(iv) Directional spectrum of the wave field. If the directional spectrum is defined by

$$F(\sigma, \theta) = \frac{1}{d\sigma d\theta} \sum_{d\sigma} \sum_{d\theta} \tfrac{1}{2} \overline{A_n^2}$$

as in Longuet-Higgins *et al.* (1963) and Nagata (1964a), then $F(\sigma, \theta)$ may be expanded as a Fourier series,

$$F(\sigma, \theta) = \tfrac{1}{2}a_0 + a_1 \cos\theta + b_1 \sin\theta + a_2 \cos 2\theta + b_2 \sin 2\theta + \ldots$$

and the coefficients a_n, b_n are given by

$$a_n + ib_n = \frac{1}{\pi}\int_{-\pi}^{\pi} e^{ni\theta} F(\sigma, \theta)\, d\theta.$$

a_n and b_n are obtained from the auto- and cross-spectra of p, u, v, w as derived from $\phi(x, y, z, t)$; e.g.

$$C_{pp}(\sigma) = \int_0^{2\pi} \frac{1}{\cosh^2 kd} F(\sigma, \theta)\, d\theta$$

which results in a value of

$$a_0 = \frac{1}{\pi}\cosh^2 kd\, C_{pp}(\sigma) = \frac{1}{\pi}\left(\frac{\sigma}{gk}\right)^2 \frac{\cosh^2 kd}{\sinh^2 kz_0} C_{ww}(\sigma). \tag{8}$$

Similarly the other Fourier coefficients are derived from the remaining spectral values to give

$$\left.\begin{aligned}
a_1(\sigma) &= \frac{1}{\pi}\left(\frac{\sigma}{gk}\right)\frac{\cosh^2 kd}{\cosh kz_0} C_{pu}(\sigma) \\
&= -\frac{1}{\pi}\left(\frac{\sigma}{gk}\right)^2 \frac{\cosh^2 kd}{\sinh kz_0 \cosh kz_0} Q_{wu}(\sigma), \\
a_2(\sigma) &= \frac{1}{\pi}\left(\frac{\sigma}{gk}\right)^2 \frac{\cosh^2 kd}{\cosh^2 kz_0}\left(C_{uu}(\sigma) - C_{vv}(\sigma)\right), \\
b_1(\sigma) &= \frac{1}{\pi}\frac{\sigma}{gk}\frac{\cosh^2 kd}{\cosh kz_0} C_{pv}(\sigma), \\
&= -\frac{1}{\pi}\left(\frac{\sigma}{gk}\right)^2 \frac{\cosh^2 kd}{\cosh kz_0 \sinh kz_0} Q_{wv}(\sigma), \\
b_2(\sigma) &= \frac{2}{\pi}\left(\frac{\sigma}{gk}\right)^2 \frac{\cosh^2 kd}{\cosh^2 kz_0} C_{uv}(\sigma).
\end{aligned}\right\} \tag{9}$$

A smoothed version of the directional spectrum may be constructed from the first five Fourier coefficients. The form of the spectrum used in this paper is due to Longuet-Higgins *et al.* (1963) and is given by

$$F_3(\sigma, \theta) = \tfrac{1}{2}a_0 + \tfrac{2}{3}(a_1 \cos\theta + b_1 \sin\theta) + \tfrac{1}{6}(a_2 \cos 2\theta + b_2 \sin 2\theta). \tag{10}$$

This form does not give negative values, but a fairly broad weighting function causes considerable smoothing of the spectrum.

If the directional spectrum is not too broad, a mean direction of travel of the wave energy may be obtained (Cartwright 1963). For a unimodal narrow angular distribution the mean direction θ is given by

$$\tan\bar{\theta} = b_1/a_1. \tag{11}$$

An estimate of the angular width of the spectrum is given by

$$\overline{(\theta - \bar{\theta})^2} = 2 - \frac{2(a_1^2 + b_1^2)^{\frac{1}{2}}}{a_0} \tag{12}$$

and the skewness s by

$$s = 2\bar{\theta} - \tan^{-1}(b_2/a_2). \tag{13}$$

5. Practical analysis of the records

(a) *Method of analysis.* Each analogue record varied in duration from 10 to 30 minutes and contained combinations of the components p, u, v, w. The traces were digitized at one-second intervals by using a semi-automatic trace-reader. The resultant time-series were analysed according to the method outlines by Blackman & Tukey (1958), i.e. auto-, co- and quadrature spectra of the components from each record were computed from the correlation coefficients of the series. Use was made of the facilities provided by the Deuce and KDF9 computers in the Computer Laboratory, Liverpool University. The first five Fourier coefficients were obtained from these spectral estimates. Tables by Wiegel (1954) were used in this procedure. A further computational stage combined the coefficients into a smoothed estimate of the directional spectrum of the surface wave energy, as represented by $F_3(\sigma, \theta)$.

(b) *Sources of error in the estimated spectra.* The main sources of error are listed below.

1. Systematic calibration uncertainty in the instruments. This source of error was estimated to give uncertainties of up to $\pm 10\%$ in each u, v, w spectrum and $\pm 5\%$ in each pressure auto-spectrum.

2. Random noise errors. The combination of instrumental, digital and computational noise introduced into the records was investigated and it was found that noise was expected to be significant in the auto-spectra only in the low and high frequency tails, i.e. $\sigma < 0{\cdot}8$ rad/s and $\sigma > 2{\cdot}2$ rad/s (where the signal level falls to near the resolution of the instrumental system).

3. Aliasing errors. The sampling interval for digitizing was $\Delta t = 1$ second. In general the records contained negligible energy contribution for $\sigma > 2{\cdot}8$ rad/s. However, comparison of the u and v spectra showed that the u component had proportionally more longer period energy. This effect is probably due to refraction of the longer waves as they move shoreward combined with the orientation of the flowmeter head. The hydrodynamic filtering reduced the risk of aliasing for these subsurface components. Thus with waves of $\sigma = 3{\cdot}6$ rad/s, recorded at 3 m above the bottom in water 6·5 m deep, the w component would be attenuated in amplitude 20 times as much as for waves of $\sigma = 1{\cdot}8$ rad/s.

4. Errors of computation. These are well covered by Munk, Snodgrass & Tucker, (1958) and can be expected to be small.

5. Errors arising from the use of hydrodynamic filter functions converting subsurface values to surface values. These errors are generally small and occur mainly in the region of the spectral peak.

6. Random errors due to finite length of record. Confidence limits may be assigned to each individual power spectrum if the record is assumed to be of a Gaussian nature. The confidence limits drawn from a χ^2 distribution show that for a 20-minute record digitized at 1-second intervals and with thirty 1-second lags there is 95% confidence that each calculated spectral value lies within 0·75 and 1·40 of the true value obtained from an infinite record. The estimation of confidence limits for the cross-spectral values is more complicated. However, a paper by Jenkins (1962) presents approximations to the variances of these quantities. It appears that the proportional variance of the transfer function between two related spectra is approximately equal to that of the individual spectral densities multiplied by the factor $\frac{1}{2}\left[\frac{1}{\gamma^2(\sigma)} - 1\right]$ where $\gamma^2(\sigma)$ is the coherency, defined as in equation (5). If $\gamma^2(\sigma) = 0{\cdot}8$, this factor is 0·125, so that in the above case the value of $\mu^2(\sigma)$ should be within $\pm 5\%$ of its true value, within 95% confidence limits.

6. Records obtained

Recording was limited to the two periods 1962 December and 1963 November–1964 April. During 1962 December, a considerable number of p, u, v records were obtained, with p at the sea bed and u, v at 0·93 m (3 ft) above it. Water depths varied between 5 m and 6 m (16–20 ft). Eighteen of these records were analysed by the method outlined previously.

During the week 1964 January 25–February 1, a large number of records of p, u, v, w were obtained. The components u, v, w were measured at 2·8 m (9 ft) above the sea-bed in water depths between 5 m and 6 m (16–20 ft). Eight records with duration 20–30 minutes were analysed. Simultaneous records of wind speed and direction at the site were obtained from the radar tower anemometer for the above sets of records.

During the period 1964 April 9–30, recordings of orbital velocity components $u(z_1)$, $u(z_2)$ and $w(z_1)$, $w(z_2)$ were obtained at heights z_1, z_2 above the sea-bed. Sixteen of these records were analysed and this enabled an investigation of the attenuation of orbital velocity with depth to be carried out. z_1 was maintained constant at 2·8 m (9 ft) and z_2 varied from 0·46 to 3·4 m (1½–11 ft). A section of a typical p, u, v, w record is illustrated in Fig. 5.

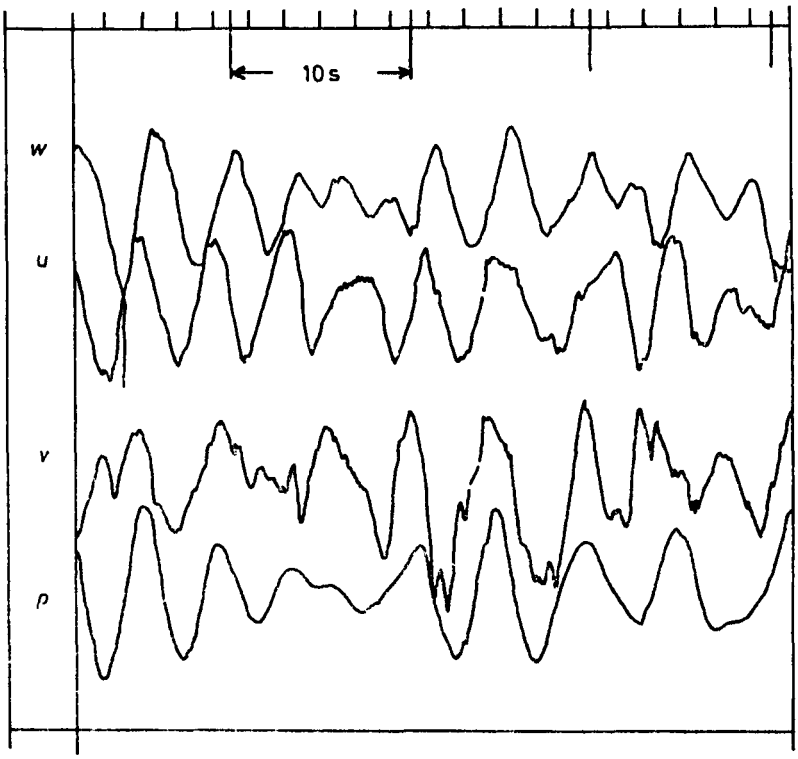

FIG. 5. Section of a typical p, u, v, w record.

7. Comparison with offshore wave observations

An estimate of the decrease in wave energy as the waves approach the shore was made by comparing a series of practically simultaneous wave records obtained at Gladstone Dock and Liverpool Bar. The Bar records were loaned by the Mersey Docks and Harbour Board, who obtained the records using a ship-borne wave recorder

mounted in the Bar Light Vessel, which lies anchored about 12 miles (20 km) seaward of Gladstone Dock in about 10 fathoms (18 m) of water.

The spectra from five sets of records taken at or near high tide were compared. The wind conditions during the recording periods were very similar with a westerly wind, 25–35 kts (13–18 m/s). In these conditions waves generally travel towards the Gladstone Shore from seaward. The ratios of the spectra for angular frequencies 1·60, 1·28, 1·06 and 0·85 rad/s (corresponding to periods of 4, 5, 6 and 7½ s respectively) were evaluated and corrected for the relative instrumental response of the ship-borne wave recorder and shore-based pressure gauge. A mean ratio for each frequency was formed from the five records, thus increasing the statistical reliability of the estimate. The square root of this mean ratio gives a fair estimate of the relative attenuation of amplitude of the waves between the Bar and the Shore. From Table 1 it can be seen that the amplitudes at the Bar are roughly twice those at Gladstone Rock. This was confirmed by an examination of the individual highest waves recorded at the two sites for a number of records. The r.m.s. surface amplitude at Gladstone Dock lay between 0·31 m and 0·45 m (computed from the pressure) for these records, and the height of the highest wave on a record was usually about six times the r.m.s. amplitude.

Table 1

Ratio of spectral energies at Liverpool Bar and Gladstone Dock

Date	Time	σ (rad/s)			
		1·60	1·28	1·06	0·85
28.1.64	0900	5·2	5·6	8·0	6·3
30.1.64	1200	4·5	5·0	6·7	6·3
31.1.64	1200	3·0	3·4	3·0	4·0
1.2.64	0000	2·5	2·6	4·8	1·8
1.2.64	1200	2·7	4·1	5·1	3·2
Average Ratio		3·6	4·1	5·5	4·3
(Average Ratio)$^{\frac{1}{2}}$		1·9	2·0	2·3	2·1

The attenuation of the wave motion between Bar and shore can probably be accounted for by two processes.

1. Attenuation due to bottom friction and wave breaking over the offshore sandbanks.

2. Refraction and diffraction of the waves as they approach the shore.

The direction of the tidal current in the Mersey Estuary appeared to affect the wave energy observed at the Gladstone Dock site. Fig. 6 provides an illustration of this effect and shows the surface elevation spectra computed from sea-bed pressure records. Records 1–4 cover the period from 1½ hours before HW (high water) to HW when the tidal current and waves were travelling in approximately the same direction. Record 5 was recorded 1 hour after HW when the ebb-tide was opposing the waves. Wind conditions were relatively constant during this period, being West 25–30 knots (13–15·5 m/s). Prior to HW the spectral energies were almost constant. However, after HW a rapid decrease in wave energy was observed for all but the lowest frequencies in the spectrum. Five other sets of records covering the same section of a tidal period in relatively constant wind conditions showed similar characteristics. It seems probable that a loss of energy will occur after HW due to the ebb-tide running over the shallow water on the sand-banks and causing a considerable steepening and breaking of the incoming waves.

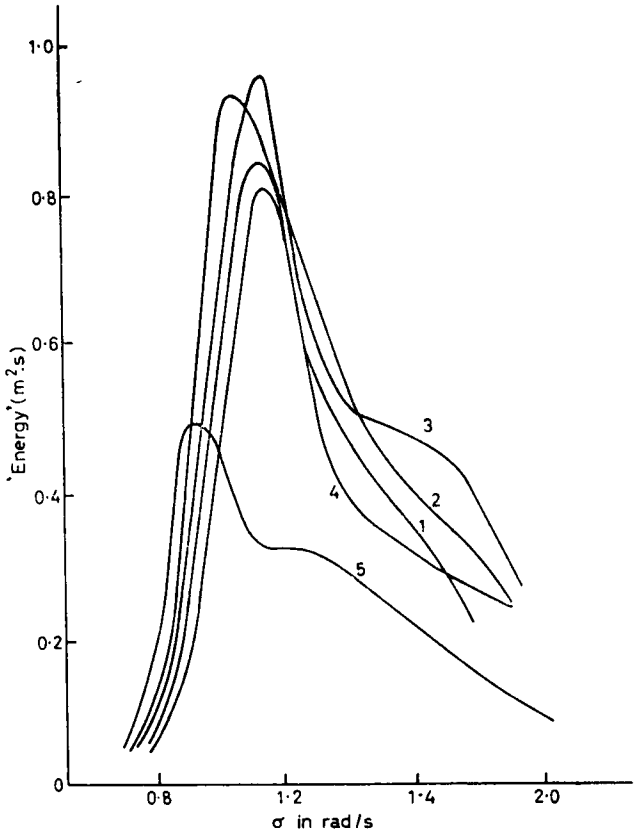

FIG. 6. Variation in wave energy at Gladstone Dock with state of the tide. Curves 1 to 4, records from 1½ h before HW to HW; curve 5, record 1 h after HW.

Table 2

Coherency $\gamma^2(\sigma)$ of p and w components (%)

σ (rad/s)	Record No. 1	2	3	4	5
0·73	06	39	35	45	27
0·84	30	68	75	73	61
0·94	82	79	86	79	75
1·05	88	82	88	81	66
1·15	82	84	83	85	80
1·25	75	83	78	87	82
1·36	74	81	84	88	81
1·46	80	85	86	88	82
1·57	88	84	85	87	84
1·67	87	83	82	88	80
1·78	80	78	81	88	76
1·88	75	65	75	86	66
1·99	71	63	61	79	60
2·09	67	56	50	80	65
2·19	73	50	54	79	54
2·30	74	35	43	42	12
2·41	64	25	36	19	20

8. Coherency, phase and transfer relations of the p, u, v and w components

(a) *p and w.* The results of an analysis of the coherency between p and w based on five records is shown in Table 2. Within the frequency range $0{\cdot}94 \leqslant \sigma \leqslant 1{\cdot}78$ rad/s the coherency exceeds 70% and in many cases is over 80%. Each of these five records was obtained in similar conditions, w being measured by 0·9 m (3 ft) above the sea bed in water depths of 4·9–6·1 m (16–20 ft). The phase difference $\phi(\sigma)$ for the five records in the range $0{\cdot}94 \leqslant \sigma \leqslant 1{\cdot}78$ is shown in Table 3. In most cases $\phi(\sigma)$ lies between 80° and 85°, with extreme values of 68° and 98°.

Table 3

Phase difference $\phi(\sigma)$ of p and w components, in degrees

σ (rad/s)	Record No. 1	2	3	4	5	Mean
0·94	68	69	87	84	77	77
1·05	69	78	88	86	78	80
1·15	78	78	90	87	77	82
1·25	84	75	98	87	78	84
1·36	84	75	88	88	81	83
1·46	85	81	84	88	84	85
1·57	85	86	81	85	85	84
1·67	85	88	79	76	81	82
1·78	88	88	76	79	77	82

Four of these five records were obtained in the same depth of water and were combined to give mean values of the transfer function $\mu^2_{pw}(\sigma)$ between p and w for parts of the individual spectra where the coherency $\gamma^2_{pw}(\sigma) \geqslant 80\%$. These mean values are compared with those calculated from equation (4) in Fig. 7. The correspondence between the experimental and theoretical values appears to be fairly good. A systematic error of up to 15% may be present in the experimental curve due to the calibration uncertainties, but this should be independent of frequency and not affect the form of the variation of C_{pp}/C_{ww} with σ.

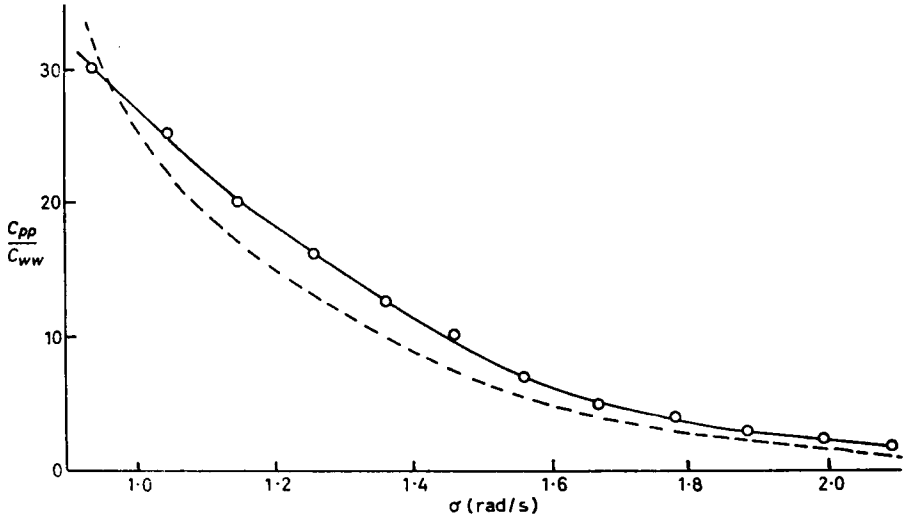

FIG. 7. Transfer function between p and w spectra:
——o—— observed values, - - - - theoretical values.

(b) *p, u and v.* A similar procedure was carried out to relate the pressure p to the u and v components. Eight records of p, u and v, obtained in similar conditions, were analysed. u and v were measured at 2·7 m (9 ft) above the sea bed when the depth of water was 5·5 m (18 ft). p was, of course, recorded on the sea bed in each case. The spectral ratio $C_{pp}/(C_{uu}+C_{vv})$ is shown for each record in Table 4.

Table 4

Ratio of pressure to u and v spectra: $C_{pp}/(C_{uu}+C_{vv})$

σ (rad/s)	Record No. 1	2	3	4	5	6	7	8
0·93	0·63	0·78	0·54	0·31	0·61	0·42	0·54	0·54
1·05	0·57	0·59	0·59	0·37	0·45	0·39	0·49	0·46
1·15	0·54	0·46	0·48	0·40	0·39	0·40	0·47	0·35
1·26	0·47	0·42	0·43	0·40	0·37	0·39	0·45	0·31
1·36	0·37	0·40	0·37	0·32	0·31	0·29	0·35	0·28
1·45	0·31	0·35	0·30	0·23	0·25	0·24	0·28	0·25
1·57	0·25	0·29	0·24	0·17	0·23	0·20	0·22	0·20
1·67	0·19	0·22	0·19	0·13	0·20	0·17	0·18	0·16
1·77	0·20	0·18	0·15	0·11	0·17	0·14	0·14	0·12
1·88	0·11	0·16	0·10	0·08	0·14	0·10	0·12	0·08
1·99	0·09	0·13	0·07	0·06	0·11	0·07	0·10	0·07
2·09	0·07	0·09	0·05	0·05	0·07	0·04	0·06	0·05

The mean value of this ratio for the eight records in the frequency range $0{\cdot}94 \leqslant \sigma \leqslant 2{\cdot}09$ rad/s is shown in Fig. 8. compared with the theoretical curve calculated from equation (3). There appears to be a significant deviation of the observed results from theory at the lower frequencies of the frequency range shown. Neglecting calibration errors, the deviation is significant at the 0·01 level for $\sigma \leqslant 1{\cdot}45$. If the calibration errors are taken as $\pm$ 15% for 90% confidence limits, the difference between the curves is still significant at the 0·05 level for $\sigma \leqslant 1{\cdot}36$. The deviation is in the sense that the pressure recorded at the bottom is greater, at low frequencies, than would be expected, on the basis of small amplitude wave theory, from the velocity components measured at a height of 2·7 m.

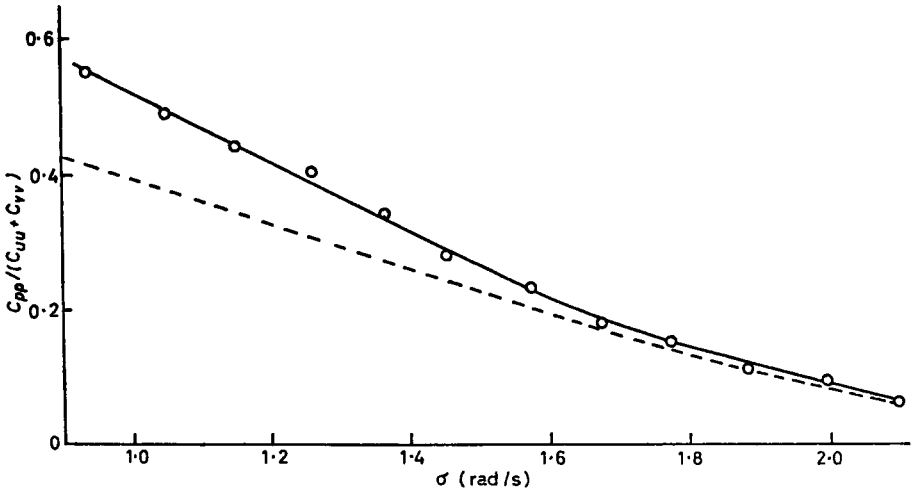

FIG. 8. Transfer function between p and u, v spectra:
——o—— observed values, - - - - theoretical values.

(c) *u components at two heights.* The coherency and transfer functions were also evaluated for two u components recorded simultaneously at different distances from the sea-bed in the same (x, y) location. The separations of the measuring heads were varied between 0·6 and 2·3 m, one unit being kept at a constant distance of 2·7 m from the sea-bed. Water depths varied from 3·7 to 4·9 ,m High coherency (> 90%) was found between u components in the peak regions of their spectra for all separations of the measuring heads. The transfer function between two u components was compared to the theoretical values expected on the basis of small amplitude wave theory (equation 2).

Table 5

Ratio of observed/theoretical transfer function for u_1, u_2 components at heights z_1 and z_2. ($z_1 = 2{\cdot}7$ m in each case)

	Record No. (value of z_2)							
σ (rad/s)	1 (0·46 m)	2	3 (0·61 m)	4	5 (1·15 m)	6	7 (1·8 m)	8 (3·4 m)
1·0	1·54	1·64	(0·97)	1·64	0·77	0·73	1·01	(2·04)
1·2	1·49	1·48	1·32	1·47	0·88	0·97	1·01	1·34
1·4	1·52	1·45	1·29	1·29	0·97	0·93	1·10	1·29
1·6	1·46	1·53	1·11	1·28	1·00	0·81	1·03	1·04
1·8	1·36	1·40	1·15	1·04	0·75	0·88	1·06	1·00
2·0	(2·06)	1·23	0·91	0·79	0·70	0·77	1·03	0·92

The ratio of the observed transfer function to the theoretical value is shown in Table 5 for eight records, for $1{\cdot}0 \leqslant \sigma \leqslant 2{\cdot}0$. In this frequency range the coherency was greater than 80%, except for those ratios which are enclosed in brackets. Four

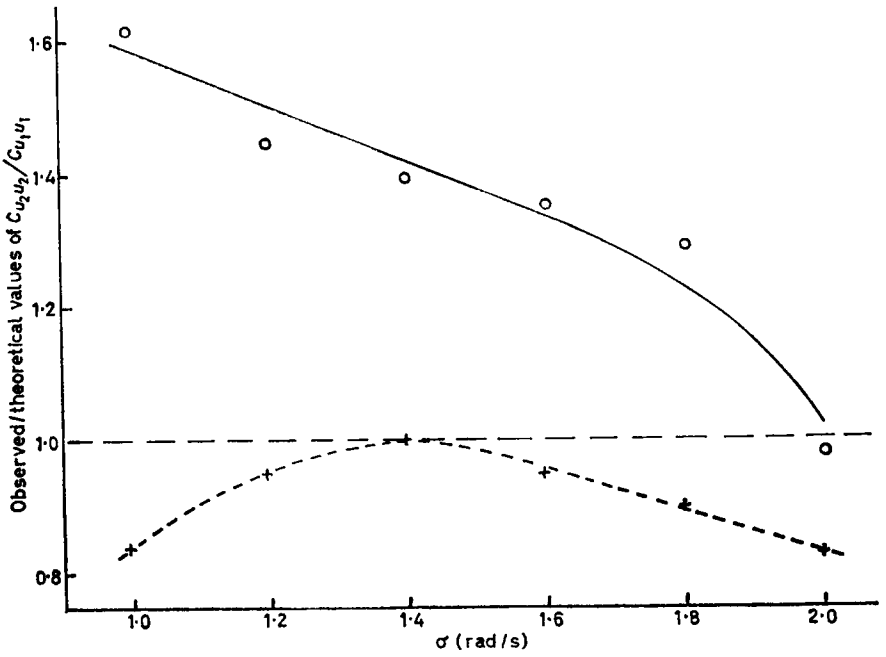

FIG. 9. Ratio of observed theoretical transfer function between u at heights z_1 and z_2: ——o—— $z_2 = 0{\cdot}46$ or 9·61 m, – – + – – $z_2 = 1{\cdot}15$ or 1·83 m.

records for which z_2 was 0·46 m (1·5 ft) or 0·61 m (2 ft) were grouped together and the mean ratios taken. Three records with $z_2 = 1{\cdot}15$ m (3·75 ft) or 1·83 m (6 ft) were grouped similarly. The mean ratios for these two groups, as functions of σ are plotted in Fig. 9. For the second group the ratio does not differ significantly from 1·00 for any value of σ. For the records at 0·46–0·61 m, however, the ratio is significantly greater than 1·00, at the 0·01 level, for all values of $\sigma \leqslant 1{\cdot}8$. The mean ratio decreases from 1·61 at $\sigma = 1{\cdot}0$ to 1·24 at $\sigma = 1{\cdot}8$.

Taking this result with that found above in section 8 (b), there is an indication that both the pressure and the horizontal velocity components are greater within about 1·0 m of the bottom than would be expected from the velocity components measured at a height of 2·7 m.

(d) *w components at two heights.* The coherency between the *w* components was lower, particularly when one component was measured close to the sea-bed. This is to be expected, since the *w* component is then small and the signal-to-noise ratio low. Table 6 shows the ratio of the observed to the theoretical transfer function for five records, in the range $1{\cdot}2 \leqslant \sigma \leqslant 2{\cdot}0$, for which the coherency was greater than 75%, with the exception of the values in brackets. Attempting to group the records, as for the *u* components, means that there are only two in each group. The mean ratios are somewhat higher for $z_2 = 0{\cdot}46$ or 0·61 m than for $z_2 = 1{\cdot}15$ or 1·83 m, but the deviations from unity are not statistically significant.

Table 6

Ratio of observed/theoretical transfer function for w_1, w_2 components at heights z_1, z_2. ($z_1 = 2{\cdot}7$ m in each case)

	Record No. (value of z_2)				
σ (rad/s)	1 (0·46 m)	2 (0·61 m)	3 (1·15 m)	4 (1·8 m)	5 (3·4 m)
1·2	(1·40)	1·24	0·80	1·24	1·21
1·4	1·16	1·21	0·73	1·20	1·14
1·6	1·13	1·38	0·93	1·21	1·02
1·8	0·95	1·42	1·00	1·22	1·08
2·0	(0·89)	1·16	0·83	1·23	1·15

(e) *Linearity of the records.* An indication of the linearity of the records is provided by a histogram showing the frequency distribution of displacements of the traces. The histograms of a typical *p*, *u*, *v*, *w* record are illustrated in Fig. 10 and the normal curve corresponding to the mean and standard deviation of each trace is superimposed. Visually there is fairly good correspondence between the experimental and theoretical distributions. A χ^2 test conducted on a considerable number of records revealed that in general the pressure distributions showed high probability of being normal (well above the 1% significance level). However, the *u*, *w* components were more variable and a considerable number lay below the 1% level. Some correlation of evidence of non-linearity with the more disturbed sea states was noticed for the *u*, *w* records, the records of waves of higher energy showing more evidence of deviation from a normal distribution.

9. The directional properties of the waves

(a) *Directional spectra.* Eighteen *p*, *u*, *v* records of the 1962 series and eight *p*, *u*, *v*, *w* records of the 1964 series were analysed for their directional spectra. The earlier records were mostly of 10 minute duration, but the later ones were of 20 minutes. These were obtained at or near high water in conditions of strong west winds during

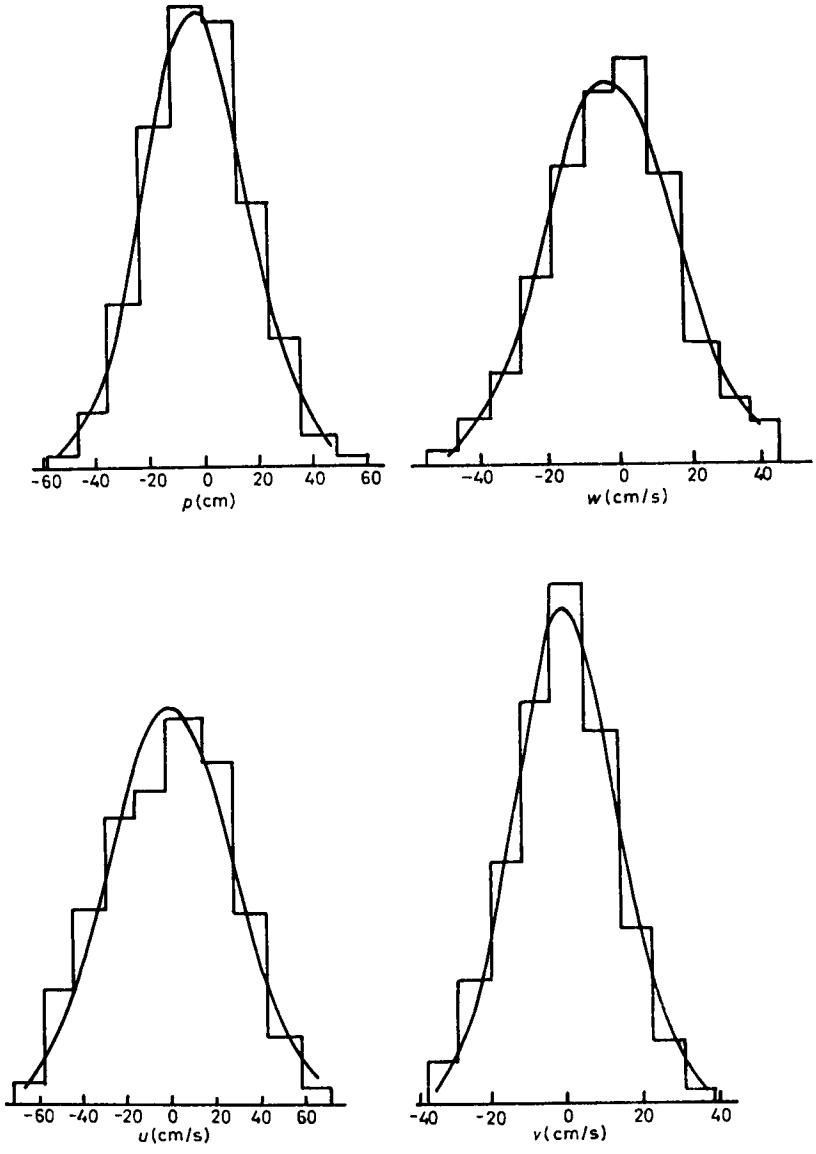

FIG. 10. Histograms of a typical p, u, v, w record.

the week 1964 January 25–February 1. The components recorded for each 20-minute record were p, u, v, w with u, v, w obtained at 2·8 m (9 ft) above the sea-bed and the water depth varying between 5 m and 6 m (16–20 ft). Analysis of the records proceeded along lines outlined in Sections 4 and 5. The individual power spectra of a typical p, u, v, w record (No. 3, 1964 January 28) are illustrated in Fig. 11. Each record exhibited similar spectra for the four components, i.e. a strongly peaked p and u spectrum with the peak lying between $\sigma = 0{\cdot}8$ and $1{\cdot}2$ rad/s. Due to the initial flow-meter alignment the magnitude of the spectral quantities relating to v are smaller than those for u. It is interesting to note the second peak in the w spectrum, occurring at approximately twice the frequency of the primary peak. This is unlikely to be due to aliasing [see Section 5(b)], but may be an indication of non-linear interaction.

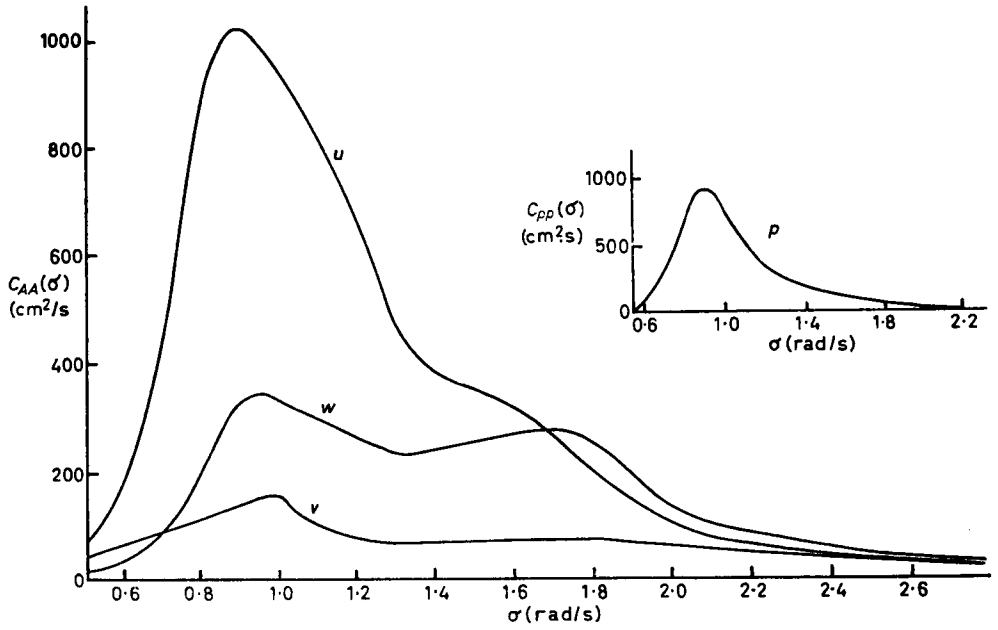

FIG. 11. Spectra of a typical p, u, v, w record.

In the theoretical equations (9) for the coefficients $a_1(\sigma)$, $a_2(\sigma)$, $b_1(\sigma)$ and $b_2(\sigma)$ in the directional spectrum, the factor $(\sigma/gk\cosh z_0)^2$ occurs because p is not measured at the same height as u and v. From equation (3) it is seen that this factor is the transfer function $C_{pp}/\{C_{uu}(z_0)+C_{vv}(z_0)\}$. As described in Section 8(b), it was found that the observed values of this function, for the lower values of σ, differed significantly from those given by equation (3). If one defines an observed transfer function $f(\sigma)$ by

$$f(\sigma) = C_{pp}/\{C_{uu}(z_0)+C_{vv}(z_0)\}$$

the equations for $a_1(\sigma)$ and $a_2(\sigma)$ may be written

$$a_1(\sigma) = \frac{1}{\pi}\cosh^2 kd f^{\frac{1}{2}}(\sigma)\, C_{pu}(\sigma),$$

$$a_2(\sigma) = \frac{1}{\pi}\cosh^2 kd f(\sigma)\{C_{uu}(\sigma)+C_{vv}(\sigma)\},$$

with similar modifications in the equations for $b_1(\sigma)$ and $b_2(\sigma)$. The coefficients $a_1(\sigma)$ etc. for the eight records of the 1964 series were computed by this method, which is self-consistent in the sense that the observed value of the transfer function between the velocity components and the pressure was used in deriving the directional spectrum.

A typical directional spectrum is illustrated in Fig. 12, which shows the value of $F_3(\sigma, \theta)$ plotted against σ for a series of values of σ. The other spectra showed similar features with a peak generally corresponding to a direction just North of West. The only evidence of bimodality occurred for $\sigma > 2{\cdot}0$ rad/s in some spectra, but at these higher frequencies the energy level is small compared with that near the energy peak. A comparison of the observed directional spectrum and the spectrum produced by the effect of the weighting function $W_3(\sigma, \theta)$ on a delta function is given in Fig. 13. At the peak frequency $\sigma = 0{\cdot}95$ rad/s the experimental curve is only slightly broader than the theoretical one, indicating that the true angular spread of the waves is quite

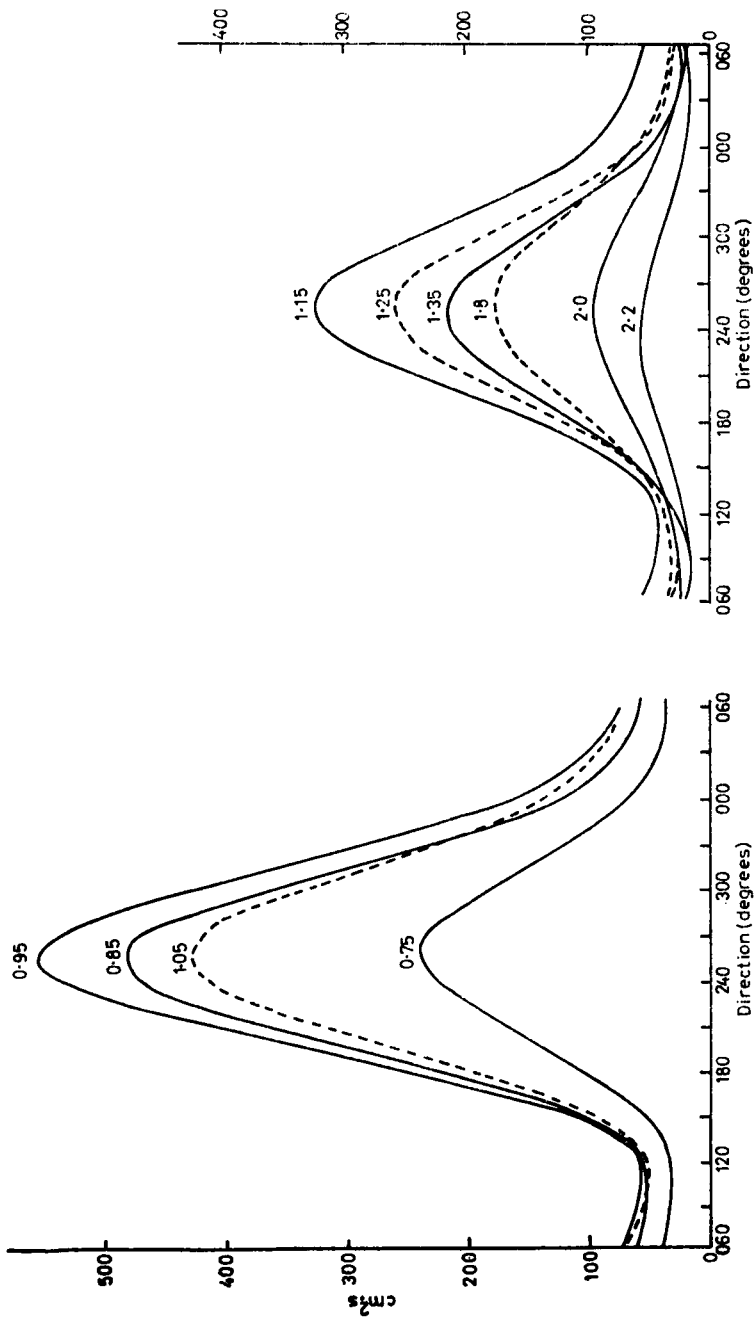

FIG. 12. Directional spectra of a typical p, u, v, w record, for a series of values of σ. The ordinate is $F_3(\sigma, \theta)$ in cm^2. s in each case and values of σ are marked against the curves.

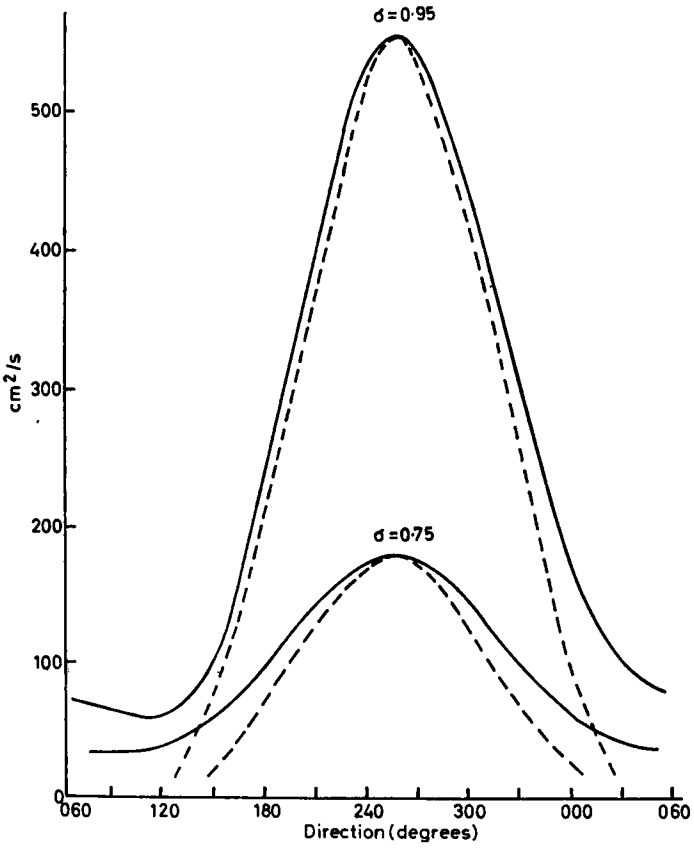

FIG. 13. Comparison of observed directional spectra and a theoretical line spectrum of zero angular width; ————, observed curves for σ = 0·75 and 0·95 (from Fig. 12); – – – –, theoretical curves.

small. However, for $\sigma = 0{\cdot}75$ rad/s the observed curve is somewhat broader, as it is also for $\sigma = 1{\cdot}8$ rad/s, on the other side of the peak, and at higher frequencies the broadening becomes more pronounced.

(b) *Mean direction and angular spread.* Estimates of the mean direction $\bar{\theta}$ of energy in the waves were found from equation (11). Table 7 gives mean values of $\bar{\theta}$ for a number of groups of records, those within each of groups A to D having been taken within a few hours in similar conditions. Similar wind and tide conditions existed for seven of the 1964 records and a mean value of $\bar{\theta}$ was obtained for them and is shown in column E. This value of $\bar{\theta}$ is representative of the site for a wind speed of 14–18 m/s (28–35 kt) and direction 280°. $\bar{\theta}$ tends to decrease with increasing σ and this may be a refraction effect, although in general one would expect the higher frequency waves to be refracted less than those of longer period.

The angular width of the distribution of energy, as represented by $\{\overline{(\theta-\bar{\theta})^2}\}^{\frac{1}{2}}$, was evaluated for each of the eight 1964 records, using equation (12), and is shown in Table 8. The general conditions during each of these records are given in Table 9. A mean value obtained for each frequency showed that the width was a minimum in the region of the spectral peak and tended to increase on either side, particularly towards the higher frequencies. Some of this increase in width may be due to loss of coherency between the pressure and velocity components.

Table 7

Mean direction of wave energy

σ (rad/s)	Direction $\bar{\theta}$ (degrees from true North) A	B	C	D	E
0·84	293	323	327	281	261
0·94	289	322	333	282	259
1·05	289	319	329	281	254
1·15	291	315	322	279	254
1·25	291	313	318	280	252
1·36	289	313	316	279	252
1·46	287	311	313	276	251
1·57	286	313	313	276	249
1·67	289	318	312	277	249
1·78	285	314	308	279	249
1·88	291	309	305	279	248
1·99	294	312	305	279	245
Mean (all σ)	289	315	317	279	252
Wind direction	320	040	020	300	280
Mean deviation (wind-waves)	31	85	63	21	28

Note: the values of $\bar{\theta}$ in columns A–E correspond to the following groups of records:

A, three records on 11.12.62;
B. three records on 13.12.62 (a.m.);
C, three records on 13.12.62 (p.m.);
D, four records on 15.12.62;
E, seven records of the 1964 series.

An estimate of the skewness of the directional spectra, given by equation (13), was obtained for each record. On the whole the skewness was small, indicating that some form of symmetric function might represent the angular distribution of energy. However, little success was encountered in attempting to fit several simple symmetric functions to the results.

Table 8

Angular width of energy distribution, in degrees

σ (rad/s)	Record No. 1	2	3	4	5	6	7	8	Mean
0·94	33	42	37	54	33	47	54	51	44
1·05	30	46	36	42	33	38	39	42	38
1·15	35	45	33	36	36	27	31	39	36
1·26	34	40	37	27	40	20	23	36	33
1·36	38	38	43	31	42	33	28	36	36
1·46	37	39	45	34	42	33	31	37	38
1·57	34	39	46	33	38	27	23	38	36
1·67	41	45	45	44	35	27	19	44	38
1·78	47	50	47	43	38	36	23	50	43
1·88	52	53	56	45	42	41	22	52	46
1·99	52	57	62	48	46	40	26	49	48
2·09	50	59	68	52	52	47	28	49	52

Table 9

Conditions during records 1–8 *of Tables* 4 *and* 8

Record No.	Date	Wind speed (m/s)	Wind direction (degrees)	Wave r.m.s. amp. (cm)	Wave T_{max} (s)
1	28.1.64	13	290	33	6·7
2	28.1.64	13	290	36	6·7
3	30.1.64	17	290	44·5	7·5
4	1.2.64	15·5	280	37·5	5·5
5	1.2.64	15·5	280	34	6·0
6	1.2.64	14·5	290	33	6·7
7	31.1.64	15·5	270	31	5·0
8	31.1.64	15·5	280	33·5	5·0

(c) *Relation to wind direction.* The correlation between the mean direction of energy in the waves and the wind direction can be seen in Table 7, where the mean wind direction is given for each group of wave records summarized in Table 7. The deviation between wind and wave direction increases as the wind becomes more northerly and hence alongshore. This is consistent with the refraction of the waves being greater under these conditions, but the complex nature of the topography would make it very difficult to investigate this point quantitatively.

10. Conclusion

The directional spectra obtained in this investigation are similar in some features to those presented by Longuet-Higgins *et al.* (1963). In the case of Longuet-Higgins *et al.*, however, the spectra represented conditions in the generating area in deep water and could therefore be used to relate the form of the spectrum to the processes of generation by the wind. In our case this could not be done, as the waves had suffered considerable modification in travelling over shallow water of complicated topography before reaching the recording site. This instrumental arrangement does provide, however, a method of studying the directional properties of the waves as they reach a particular coastal position. In a situation with simpler topography, e.g. a sea-bed sloping uniformly away from the shore, a correction could be applied to the observed spectrum to transform it to the spectrum of the waves in deep water. Further experiments are being carried out in this Department with these points in view.

Another application of this technique would be to the study of changes taking place in the properties of the waves as they approach the breaking point and in the breaker zone itself. In the present work, although the water was comparatively shallow, the ratio a/d, i.e. the wave amplitude to the depth of water, did not exceed 0·2. Although there was some evidence of non-linear effects, as mentioned in Section 8(e), in general these were small.

Acknowledgments

The authors wish to acknowledge the valuable assistance of Mr J. Atkins in setting up the equipment and making the observations. They are also pleased to acknowledge the help of the Mersey Docks and Harbour Board, who provided the site and made various facilities available there, and the National Institute of Oceanography, who provided the pressure recorder on loan for this work.

Oceanography Department,
University of Liverpool.
1966 *March.*

References

Barber, N. F., 1963. *Ocean Wave Spectra*, pp. 137–150. Prentice-Hall.
Blackman, R. B. & Tukey, J. W., 1958. *The Measurement of Power Spectra*. Dover.
Bowden, K. F. & Fairbairn, L. A., 1956. *Proc. R. Soc.*, A, **237**, 422–438.
Cartwright, D. E., 1963. *Ocean Wave Spectra*, pp. 203–218. Prentice-Hall.
Cartwright, D. E., 1962. *The Sea*, Vol. 1, pp. 567–568. Interscience.
Cartwright, D. E. & Smith, N. D., 1964. *Buoy Technology*, pp. 112–121. Marine Technology Society, Washington.
Cartwright, D. E., Tucker, M. J. & Catton, Diana, 1962. *Trans. Soc. Instrum. Technol.*, **14**, 1–16.
Cote, L. J. *et al.*, 1960. *Met. Pap. N.Y. Univ.*, Vol. 2, No. 6.
Harris, M. J. & Tucker, M. J., 1963. *Instrum. Pract.*, **17**, 1055–1059.
Howe, M. R., 1960. Ph.D. Thesis, University of Liverpool.
Inman, D. L. & Nasu, N., 1956. *Tech. Memo. Beach Eros. Bd U.S.*, No. 79.
Jenkins, G. M., 1962. *Time-Series Analysis*, pp. 267–276. Wiley.
Lamb, H., 1932. *Hydrodynamics*, 6th edition. Cambridge University Press.
Longuet-Higgins, M. S., 1962. *Proc. R. Soc.*, A, **265**, 286–315.
Longuet-Higgins, M. S. & Barber, N. F., 1946. ARL/R.I/102.22/W, Admiralty Research Laboratory, Teddington, Middlesex.
Longuet-Higgins, M. S., Cartwright, D. E. & Smith, N. D., 1963. *Ocean Wave Spectra*, pp. 111–132. Prentice-Hall.
Lukasik, S. J. & Grosch, C. E., 1963. *J. geophys. Res.*, **68**, 5689–99.
Miller, R. L. & Zeigler, J. M., 1964. Proceedings of the Ninth Conference on Coastal Engineering, *Am. Soc. Civ. Engrs*, pp. 103–122.
Munk, W. H., Miller, G. R., Snodgrass, F. E. & Barber, N. F., 1963. *Phil. Trans. R. Soc.*, A, **255**, 505–584.
Munk, W. H., Snodgrass, F. E. & Tucker, M. J., 1958. *Bull. Scripps Instn Oceanogr. tech. Ser.*, **7**, 283–362.
Nagata, Y., 1961. *Rec. oceanogr. Wks Japan*, **6**, 53–62.
Nagata, Y., 1964a. *J. oceanogr. Soc. Japan*, **19**, 169–181.
Nagata, Y., 1964b. *J. oceanogr. Soc. Japan*, **20**, 57–70.
Nagata, Y., 1964c. *J. oceanogr. Soc. Japan*, **20**, 71–80.
Nagata, Y., 1964d. *Coastal Engineering in Japan*, Vol. 7, pp. 11–30.
Wiegel, R. L., 1954. *Gravity waves, tables of functions*, Council on Wave Research. Engineering Foundation, Berkeley, California, U.S.A.